

A potentiometric tattoo sensor for monitoring ammonium in sweat

Cite this: *Analyst*, 2013, **138**, 7031

Tomàs Guinovart,^{ab} Amay J. Bandodkar,^a Joshua R. Windmiller,^{ac} Francisco J. Andrade^{*b} and Joseph Wang^{*a}

The development and analytical characterization of a novel ion-selective potentiometric cell in a temporary-transfer tattoo platform for monitoring ammonium levels in sweat is presented. The fabrication of this skin-worn sensor, which is based on a screen-printed design, incorporates all-solid-state potentiometric sensor technology for both the working and reference electrodes, in connection to ammonium-selective polymeric membrane based on the nonactin ionophore. The resulting tattooed potentiometric sensor exhibits a working range between 10^{-4} M to 0.1 M, well within the physiological levels of ammonium in sweat. Testing under stringent mechanical stress expected on the epidermis shows that the analytical performance is not affected by factors such as stretching or bending. Since the levels of ammonium are related to the breakdown of proteins, the new wearable potentiometric tattoo sensor offers considerable promise for monitoring sport performance or detecting metabolic disorders in healthcare. Such combination of the epidermal integration, screen-printed technology and potentiometric sensing represents an attractive path towards non-invasive monitoring of a variety of electrolytes in human perspiration.

Received 4th September 2013
Accepted 26th September 2013

DOI: 10.1039/c3an01672b

www.rsc.org/analyst

1. Introduction

Ammonium is present in blood mostly as a result of the breakdown of proteins.¹ For this reason, the determination of the levels of this cation in plasma provides extremely relevant physiological information related to the metabolic state of the individual, dietary conditions, or even liver malfunctions. During exercise, for example, ammonium concentration varies when changing from aerobic to anaerobic state.^{2,3} Also, it has been shown that diets with low levels of carbohydrates may lead to temporary increased levels of ammonia in plasma, which is sometimes evidenced as an ammonia smell in sweat. Last, but not least, since the liver converts ammonia to urea prior to its excretion, high ammonia levels can be used as markers of hepatic disorders, such as hepatitis or cirrhosis.⁴ All in all, monitoring the levels of ammonium may provide a wealth of information, which ranges from the improvement of the sport performance and monitoring metabolic state to the screening of the health status of individuals. Unfortunately, monitoring ammonium in plasma requires the collection of blood samples, which is a serious limitation during exercise or military activities.

On the other hand, ammonium is excreted through sweat by non-ionic diffusion from plasma,⁵ and many studies have shown that the ammonium levels in sweat can be directly correlated with its concentration in plasma. Czarnowski *et al.* examined the relationship between ammonia and urea levels in plasma and ammonium concentration in sweat. Their studies suggest that ammonia in plasma is the main source of ammonium in sweat.⁶ Subsequent studies of ammonium secretion *via* sweat have been carried out through physical exercise such as running, where sweat was collected with gauze pads. The measurements in the collected sweat of the total amount of nitrogen excreted (urea, ammonium and amino acid loss) concluded that the difference of nitrogen loss by comparing both methods is relatively small.⁷ Other tests performed under submaximal cycling exercise (and comparing the results of ammonium with both, urea and lactic acid) suggested that ammonium is secreted through sweat during short-term exercise on the onset of sweating.⁸ Yuan *et al.* studied the effect of one year non-specific program on the ammonia threshold, which was uniquely correlated to endurance time.⁹ Also, studies performed with rugby players, where the ammonium levels in sweat were monitored before, during and after the game, showed a significant increase while playing the match. This was also correlated with the concentration of ammonia in blood, which showed an increment almost three times higher.¹⁰ Last, but not least, studies of the ammonium levels in sweat were also performed with a low-carbohydrate (LC) and normal diet, in both cases combined with non-exhausting exercise. The clear

^aDepartment of Nanoengineering, University of California San Diego, La Jolla, CA, 92093-0448, USA. E-mail: josephwang@ucsd.edu

^bDepartament de Química Orgànica, Analítica i Nanosensors, Universitat Rovira i Virgili, C/Marcel·lí Domingo s/n, Tarragona, 43007, Spain. E-mail: franciscojavier.andrade@urv.cat

^cElectrozyme LLC, Executive Square (Suite 485), San Diego, CA 92037-4225, USA

increase of ammonium in LC diet confirms the hypothesis of ammonia in plasma as the main source of ammonium in sweat.¹¹ In summary, the secretion of ammonium in sweat can be used as an indicator of the metabolic breakdown of proteins, providing extremely relevant information in many different situations such as the change from aerobic to anaerobic exercise (*i.e.*, the point where carbohydrates sources have been depleted and the metabolism starts to break down proteins from the body due to mainly by high-intensity exercise)⁸ when monitoring sport performance.

From an analytical point of view, one of the major barriers to monitoring the concentration of ions in sweat lies in the sampling step. The traditional approach involving gauze pads to collect sweat is tedious, time consuming, and subject to errors, since factors affecting the evaporation, contamination of the sample, *etc.*, must be strictly controlled. For this reason, wearable devices that can directly monitor the sweat composition have emerged as a more attractive option. Diamond *et al.* developed optical and potentiometric sensors to monitor pH and sodium levels in sweat. Their results clearly demonstrated the value of monitoring electrolytes in sweat, although the devices presented were not fully portable.¹² Curto *et al.* developed a micro-fluidic wearable device based on colorimetric imaging for continuous pH monitoring with the use of a smartphone.¹³ Coyle *et al.* utilized a textile-platform to monitor pH, sodium, sweat rate and conductivity, although the same issues of portability were not discussed.¹⁴ Wang *et al.* developed different approaches for flexible screen-printed electrodes in wearable devices.^{15,16} Guinovart *et al.* recently reported a method to turn conventional cotton yarns into ion-selective electrodes using carbon nanotubes and polymeric membranes.¹⁷ These approaches provide interesting paths to build fully wearable sensors incorporated into garments that will eliminate the troublesome sampling step.

From lab-based to portable devices, and from portable to fully embedded sensors, there is a clear trend towards the incorporation of devices into objects to generate chemical information. This trend responds to the growing needs to generate analytical systems that are not only robust, but that also adapt to the end-users needs, eliminating any complicated steps and disruptions to their routines. For this reason, an approach that is gaining considerable momentum in this field is the epidermal integration of the sensors through temporary tattoos. Rogers *et al.* reported the development of an electronic epidermal platform to monitor several physiological parameters, including temperature, heart rate and brain activity.¹⁸ Wang's team developed tattooed screen-printed electrochemical sensors to monitor several environmental and physiological parameters. These "epidermally integrated" amperometric platforms were used to detect molecules such as TNT,¹⁹ lactate²⁰ and more recently a tattooed potentiometric platform to monitor epidermal pH.²¹

The present work demonstrates the development and characterization of a tattooed potentiometric cell to monitor ammonium in sweat. A screen-printed temporary-transferred tattoo paper is prepared using an ammonium-selective polymeric membrane (based on the nonactin ionophore) and

solid-state reference electrode. Thus, the work combines the previously reported advantages of the tattooed electrochemical sensors,¹⁹ with the unique features of solid-state potentiometric sensors, such as extremely low power consumption, simplicity of operation and wide linear dynamic ranges (among many others). Furthermore, polyvinyl butyral (PVB) has been employed for the first time as a solid-state reference membrane in a wearable device. The combination of this polymer with saturated NaCl forms nanopores on the surface that allow the generation of a stable phase-boundary interface between membrane and solution.²² The resulting tattoo sensor shows good stability and Nernstian response over 3 orders of magnitude (10^{-4} to 10^{-1} M). The construction and operation of the sensor are described, and factors affecting the analytical performance are discussed. Such combination of the epidermal integration, screen-printed technology and potentiometric sensing shows an attractive path towards the full integration of chemical sensors in several areas, such as telehealth or the improvement of sport performance.

2. Experimental section

2.1 Reagents

Analytical grade salts of ammonium chloride and sodium chloride (99.5%), nonactin (ammonium ionophore I), 2-nitrophenyl-octyl ether (*o*-NPOE) with >99% purity and high molecular weight poly(vinyl chloride) were all purchased from Sigma-Aldrich (St. Louis, MO). Tetrahydrofuran (THF) with HPLC grade was purchased from Fisher Chemical (Fair Lawn, NJ). Methanol (99.8% anhydrous) was purchased from Aldrich Chemical Co. Inc. (Milwaukee, WI). Polyvinyl butyral (PVB) B-98 was purchased from Quimidroga S.A. (Barcelona, Spain).

Carbon fibers (8 mm diameter, 6.4 cm length, 93% purity) were procured from Alfa Aesar (Ward Hill, MA) and their length was reduced to 0.5 mm (by cutting with a sharp blade) followed by thorough cleaning in acetone.

2.2 Electrochemical measurements

Electromotive force (EMF) was recorded using a high-input impedance (>100 G Ω , 3 μ V resolution) data acquisition device (AUTOLAB Type III model μ 3AUT070676 – Eco Chemie, B. V., Utrecht, The Netherlands) and NOVA software (0.01 s integration time, v.1.8, The Netherlands) as a measuring interface, at room temperature (22 $^{\circ}$ C) without any ionic strength adjuster. The EMF values were corrected using the Henderson equation for the liquid-junction potential and the activity was calculated by the Debye–Hückel approximation. Doubly deionized water (18.1 M Ω cm $^{-1}$) was employed in all the experiments.

Stretching and bending tests of the tattoos were carried out by using a mechanical testing instrument (INSTRON – 5982 dual column floor model – Norwood, MA) in combination with Instron Bluehill software.

2.3 Reference and ion-selective membranes

A solid-state reference membrane was made using a 10 wt% polyvinyl butyral (PVB) in methanol solution containing

saturated NaCl. The cocktail was made by dissolving 78.1 mg of PVB and 50 mg NaCl in 1 ml of methanol. The mixture was vigorously shaken for 30 minutes in an AJT instruments ultrasonic bath (75 Hz). Once used, the cocktail is kept at room temperature and remains stable for 2 weeks.

The ammonium-selective membrane contains 0.2 wt% of nonactin, 69.0 wt% of 2-nitrophenyl octyl ether (*o*-NPOE) and 30.8 wt% of poly(vinyl chloride), as described elsewhere.²³ The membrane was prepared by dissolving 100 mg of all the mixture in 1 ml of THF. The cocktail was vigorously shaken for 30 minutes in an ultrasonic bath. Once it is used, the cocktail is kept in the fridge at 4 °C, and remain stable for 2 weeks.

2.4 Fabrication of the tattoo sensor

Details on the construction of a tattoo sensing platform can be found elsewhere.^{19–21} The tattoo design for the development of the potentiometric cell sensor in this work was chosen to be a “flower-shaped”, where the silver/silver chloride (Ag/AgCl) layer – right petal – is the reference electrode and the interior circle is the ion-selective electrode (see Fig. 1). At the end of each electrode there is a part where the tattoos can be connected to the potentiostat. In order to facilitate the connection, a silver conductive epoxy material (MG-Chemicals, Cat. no. 8331-14G) was used to extend each electrode in order to facilitate the connection to the high-input voltmeter.

The shape of the cell was designed in AutoCAD (Autodesk, San Rafael, CA) and outsourced for fabrication on 75 µm thick stainless steel stencils (Metal Etch Services, San Marcos, CA). A separate stencil pattern was developed for each layer (Ag/AgCl, carbon and insulator). An MPM-SPM semi-automatic screen printer (Speedline Technologies, Franklin, MA) was employed

for the printing of the tattoo. A4-sized sheet of temporary transfer tattoo paper (Papilio, HPS LLC, Rhome, TX) was used as a substrate.

In order to increase the tensile strength of the printed electrodes, 0.04% chopped carbon fibers (CFs) were dispersed in the inks and homogenized thoroughly.¹⁹

The construction of the sensor involves several steps. First, a transparent insulator layer is printed on a tattoo paper sheet to facilitate the release in the last step. Thereafter, a Ag/AgCl layer with a longer right petal is printed. Then the printing process is followed by the carbon layer with the interior circle and the longer left petal. Finally another blue insulator layer – which represents the surrounding “leaves” – is printed. After each layer, the inks were cured for 15 min at 90°. At the end of the process, sensors were cut into individual tattoos for a single use (see Fig. 1A). A single tattoo has a dimension of 15 × 15 mm for the smallest version up to 40 × 40 mm for the largest version.

Once the tattoo is screen-printed and cured, the next step the incorporation of the reference and ion-selective membranes. To do this, a total of 5 µl of the reference membrane were drop-casted covering the entire right petal and let to dry overnight. This drying step is essential in order to have a stable potential in the potentiometric measurement since at shorter times of drying the calibration shows a relative drift of the potential. It has been already demonstrated with the polymer used in this work (PVB) that the drying process is essential to obtain a stable and reproducible potential.²² While the reference membrane is being dried, the ammonium ion-selective membrane can be cast onto the inner circle of the flower. This step was also optimized in order to get a stable and reproducible ISE by drop-casting different amounts of the ion-selective membrane cocktail. The final volume was of 15 µl, applied in steps of 5 µl each

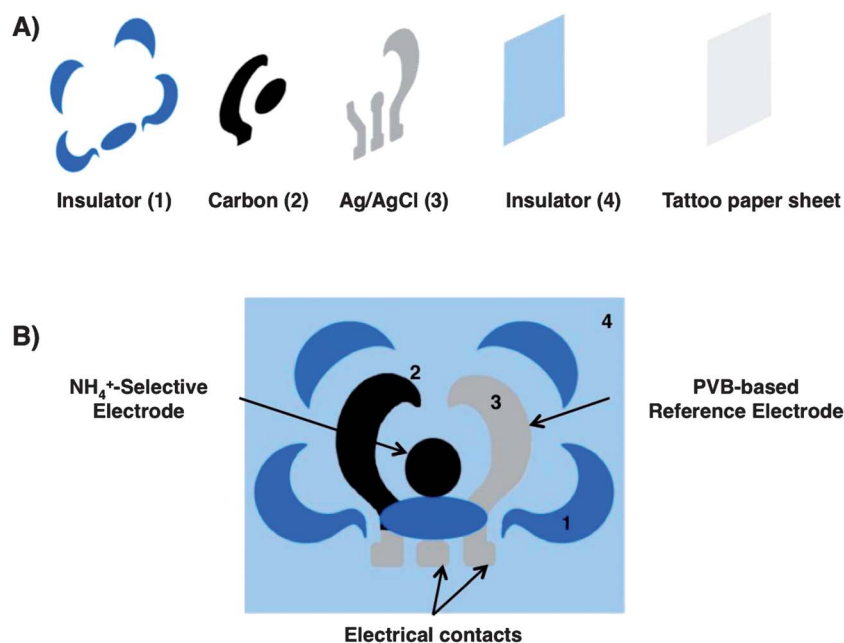


Fig. 1 Layer-by-layer fabrication of the potentiometric tattoo sensor. (A) The process starts by adding a release layer in a tattoo paper sheet. Ag/AgCl, carbon and insulator layers are screen-printed onto the release layer to get the flower tattoo. (B) Both reference and ion-selective membranes are deposited onto the electrodes area.

(see Fig. 1B). All the experiments were carried out without any previous conditioning of the membranes, so that all the studies in this work have been repeated at least three times in order to obtain a good reproducibility in terms of slope and intercept.

A protective layer from a transparent sheet was attached on top of the tattoo, and is removed by peeling off in order to expose the electrodes when required. The tattoo is thus applied on the substrate and the protective layer with the square is peeled off and attached an insulating tape onto alumina foil to avoid the contact of the sample with the conductive parts.

3. Results and discussion

3.1 Characterization of the sensor

The performance of the new ammonium potentiometric tattoo sensor was evaluated by recording the electromotive force (EMF) upon changes of activity of the analyte by using standard solutions of varied concentrations. It must be mentioned that both reference and working electrode were not conditioned before starting the calibrations, although it is very-well known that the first contact of solution with the reference membrane and the ion-selective membrane is very important²⁴ for the performance of these types of sensors. Previous studies have shown that an all-solid-state reference electrode can be developed using a PVB polymer in combination with a cocktail of salts (NaCl and AgNO₃).²² An improvement to this approach has been introduced in this work by taking advantage of the screen-printed layer of Ag/AgCl that forms part of the tattoo. Thus, a layer of the reference cocktail composed only by the PVB polymer and saturated NaCl is drop-casted on the reference petal. The results of this work demonstrate that this platform can be also used as a reference electrode.

A calibration of the tattoos-sensors was performed by recording the EMF *versus* the time and changing the activity of ammonium (Fig. 2) by adding drops of solution on top of both electrodes. The results show that the tattoo-sensor offers a relatively fast change of EMF upon changing the activity, reaching the steady-state response in about 5 s.

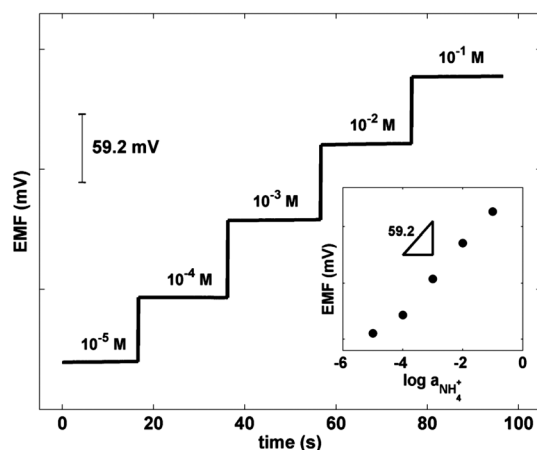


Fig. 2 Potentiometric time trace upon changes of ammonium concentrations. Inset: EMF dependence vs. $\log(a_{\text{NH}_4^+})$ for nonactin-based membranes.

Such response time seems appropriate for monitoring physiological parameters, since the change of ammonium concentration during sweating is progressively increasing whenever the body starts burning proteins instead of carbohydrates (due to the depletion of sugars when changing from aerobic to anaerobic state). This tattoo sensor shows a linear range from 10^{-4} M to 0.1 M with a Nernstian slope of 59.2 ± 0.3 mV/ $\log a_{\text{NH}_4^+}$ (5.21% RSD, $n = 5$) (see inset in Fig. 2). This range covers the typical ammonium levels in sweat.⁶ The calculated limit of detection is $10^{-4.9}$ M, which is comparable to the values reported by previous studies using a similar ion-selective membrane.²³

Selectivity is another important parameter to evaluate, since sweat is usually rich in other ions, such as K^+ , which is known to be an interference for the ISE determination of ammonium.²⁵ Selectivity values were calculated by separate solution method (SSM) for the two most abundant cations in sweat, namely Na^+ and K^+ . The results can be seen in Table 1.

The data shows that the performance of the tattoo-ISE is very close to conventional electrodes. Typical values of K^+ in sweat fall within the 0.2 to 6 mM range and for Na^+ from 30 to 100 mM. Considering NH_4^+ levels in the 0.1 to 1 mM (ref. 6) range, these constants suggest that the problems of interferences should not be a serious issue.

The repeatability of the response of a single sensor was evaluated by performing several calibration plots. The results for 5 repetitions yielded an average slope value of 58.7 ± 0.8 mV/decade (1.37% RSD) and an intercept of 317 ± 3 mV (0.89% RSD). Additionally, several experiments were conducted in order to evaluate the reproducibility of the response for different tattoo-sensors. In this case, the response of 5 different tattoos was evaluated yielding a slope value of 57.5 ± 1.4 mV/ $\log a_{\text{NH}_4^+}$ (2.38% RSD) and an intercept of 489 ± 35 mV (7.14% RSD).

From an analytical and also a practical perspective, these values evidence some of the most attractive features as well as some limitations of the proposed approach in real scenarios. First, one of the most interesting features of potentiometry is the inherently constant value of the sensitivity (*i.e.*, the Nernstian response). This an interesting feature for decentralized measurements (*i.e.*, determinations performed in large scale outside the lab), since having a method with a known sensitivity that is virtually independent of the operational parameters reduces the complexity of operation and the uncertainty of the results. Corrections in temperature factor should be considered in the future when developing real applications. It should be stressed, however, that a change from lab temperature (298 K) to body temperature (approximately 310 K) should give

Table 1 Selectivity values obtained experimentally and in literature for the nonactin-based polymeric membrane

Analyte	$\log K_{\text{NH}_4^+Y}^a$	$\log K_{\text{NH}_4^+Y}$ (ref. 23)
K^+	-1.8	-1.6
Na^+	-2.9	-2.6

^a Results obtained in this work.

according to Nernst equation a variation of about 4% in the slope, which is close to the experimental error previously described.

Another important factor is the variability of the intercept, which is a common problem in wearable potentiometric devices that needs to be overcome by calibration. Rius-Ruiz *et al.* demonstrated that a single point calibration was enough in these cases to provide reliable results.²⁶ Whether this calibration can be performed at the final stage of the manufacturing process and can be reliably used later depends on shelf stability of the sensors and other type of assessments that go beyond the scope of this work. Note that the reproducibility of the intercept reported above was calculated for different tattoos made within the same production batch. Larger values are obtained when comparing different batches.

Because of the progressive increase of ammonium when sweating, it is important to test the changes on the response of the electrode when ammonium activity fluctuates, in order to evaluate hysteresis effects (carry-over test) when ammonium fluctuations are taking place. To study this effect, tattoo sensors were subjected to successive changes in the ammonium concentrations without any conditioning or rinsing the devices between changes of the solutions. Fig. 3 shows the results of this carry-over test to ISE sensors by using solutions of alternating ammonium concentrations. Additionally, a similar test was performed using a conventional filter papers soaked with solutions of different concentrations, in an attempt to mimic the skin and the fluctuations of ammonium in sweat. This carry-over test was repeated several times until a more reproducible and stable EMF pattern was obtained due to, in part, the use of non-conditioned membranes. This phenomenon may be, in part, due to the reference electrode, which also needs to be stabilized in contact with a solution, as was reported earlier.²² This carry-over test demonstrates the viability of using these sensors when rapidly fluctuating ammonium levels take place. Also, the reproducible pattern obtained with the soaked filter paper suggests a potential way to pre-calibrate or validate the sensor response in a simple way in future practical applications. It should be noted that when the electrodes are in contact with the soaked paper, a slightly slower response time for the system

is obtained, especially at higher concentrations (see Fig. 3B). For that reason there is an apparent drift at higher concentrations, which disappears once the signal has reached the steady state.

A key feature of wearable devices is the ability to work under rough conditions, particularly under mechanical stress, without significantly affecting the response. This is particularly true for sensors worn on the skin, which can be deformed during their use. Stretching and bending tests of sensing tattoos applied to a GORE-TEX[®] textile that mimics the skin have been reported in previous studies.²⁰ This test is particularly relevant in real applications, such as monitoring the sport performance of athletes during exercise, when extreme and repeated movements of the muscles are common. In order to test the stretching effect, the textile containing the tattoo was anchored between two forceps that move away up to 5 mm, at speed of 1 mm s^{-1} . This process was repeated up to 40 times, calibrating the sensor after every 10 stretching cycles from 10^{-5} to 0.01 M . The results show a final sensitivity of $60.1 \pm 1.4 \text{ mV/decade}$ (2.34% RSD) and an intercept of $411 \pm 4 \text{ mV}$ (6.91% RSD). It has to be noted that in this case it was not possible to stretch more times the tattoo since the tattoo presents a more delicate part in the reference electrode which is damaged after 40 times, leading to a non-Nernstian response. Future efforts, focusing on the design, materials and manufacturing process, may help to improve durability of the sensors under these stringent mechanical deformations.

In a different experiment, the bending was tested anchoring once again the GORE-TEX[®] textile between the two forceps, but in this case twisting back and forth the textile at angles close to 180° . This test was repeated up to 100 times, and calibration of the sensor was performed after 10 bending cycles. In this case, the sensitivity obtained was $59.2 \pm 1.5 \text{ mV/decade}$ (2.60% RSD) and an intercept of $408 \pm 12 \text{ mV}$ (2.97% RSD). Therefore, in this case it is clear that the tattoo is not affected by any bending process after 100 times. The baseline shifting in both Fig. 4A and B is due to the conditioning processes (as in the case of carry-over test). The baseline is always more reproducible after calibrating the sensor many times (except in the case of stretching, where the sensor was broken). All these results provide useful information when developing procedures for the use of these

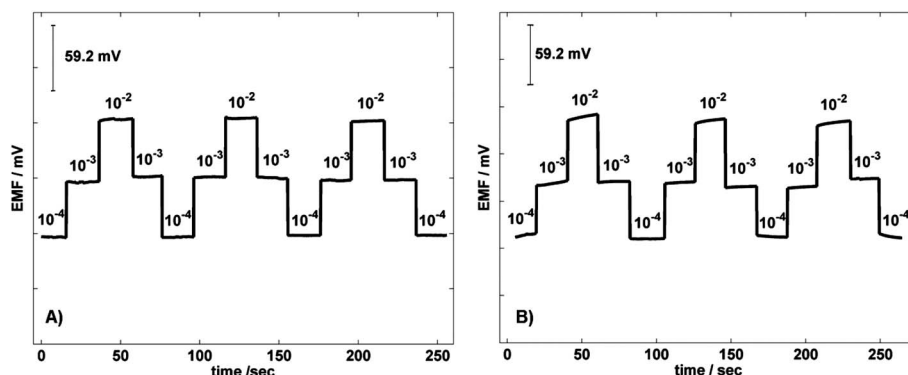


Fig. 3 Carry-over test within 10^{-4} to 10^{-2} M range in potentiometric tattoo sensor. (A) Test with the sample solution in contact with the electrodes, (B) test with a filter paper soaked at different concentrations and placed on top of sensor.

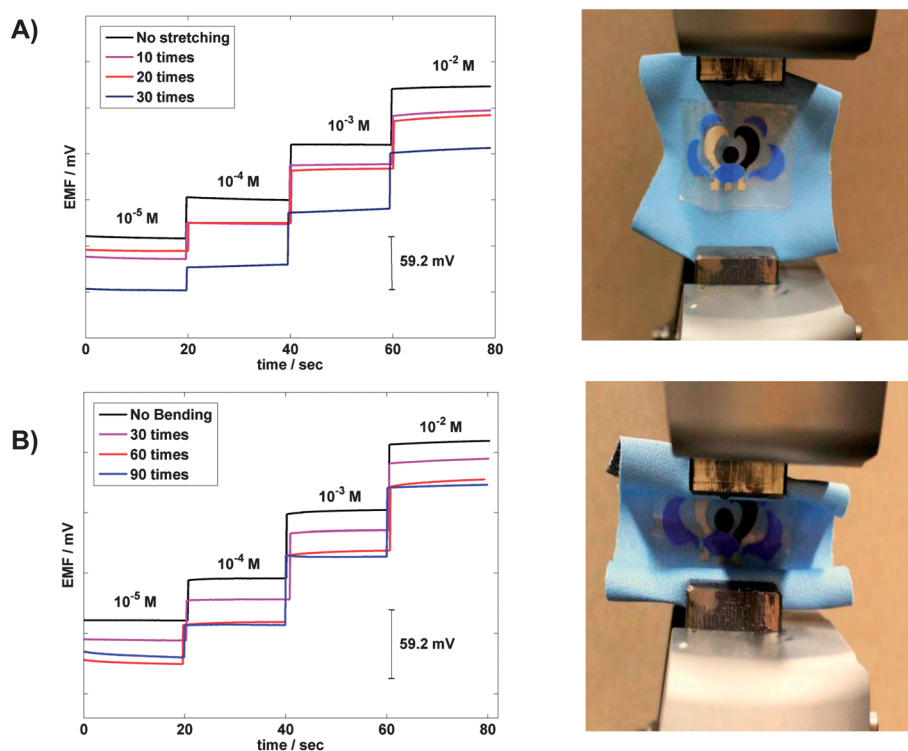


Fig. 4 Effect of mechanical stretch and bend of the tattoo potentiometric sensor. (A) Left: calibration curves from 10^{-5} to 10^{-2} M at each 10 stretches. Right: tattoo applied on GORE-TEX[®] and being stretched. (B) Left: calibration curves from 10^{-5} to 10^{-2} M at each 30 bends. Right: tattoo applied on GORE-TEX[®] and being bent.

devices in real scenarios, since the locations in the body where to monitor sweat will be differently affected by the movement of the muscles. Tests where measurements were performed during the stretching/bending were not performed in this work. Future work including these type of measurements could be interesting to evaluate their effect on real-time monitoring.

3.2 On-body testing

Once the sensor is completely characterized and its performance has been shown to be well within the sweat physiological range, preliminary experiments were performed testing the sensor directly on the skin. In this work the tattoo sensor was only placed on the shoulder (in order to avoid sharp movements, see Fig. 5A) of several volunteers doing physical activity at different levels. Once placed directly on the skin, the sensor shows some practical problems, particularly regarding the contact between the electrodes. In order to solve those issues, small changes to adapt the sensor were performed. First, two strips made of Kapton[®] (an electrically insulating polyimide film widely used in flexible electronics) were placed on both sides of the tattoo. This creates a “path” where the sweat is able to flow-through keeping the electrical contact between both electrodes through the solution. Additionally, a filter paper at the end of the path is used as a ‘sink’ to retain the sweat while facilitating the flow (see Fig. 5B). This design of the electrochemical cell provides a path where sweat can flow-through, to ensure a proper sensor operation, even when volunteers have higher sweat rate.

The sensor is calibrated at least 3 times before the modification with the path and placed onto the skin. In order to place the tattoo on the skin, wires in contact with carbon ink screen-printed onto polyethylene terephthalate (PET), cured at 90 °C for 15 min, only in one side are used. These carbon connections were attached to the tattoo with silver conductive epoxy and covered with an insulating commercial ink to avoid the contact of sweat with the connections. To ensure a proper attachment of the tattoo, an extra adhesive tape is placed on the skin. This allows both electrodes to be in good electrical contact with the tattoo without interfering with the measurements.

In the experiment, a stationary cycling routine of 30 min exercise, with 3 min of cooling down and 3 min more of a complete stop were used. Each volunteer ingested mineral water during the exercise and either increase the load while cycling or sprinting every 5 min to force the body to come into an anaerobic state.

The results of these experiments are displayed in Fig. 5C. First, a noisy signal due to the movements and the effect of having the sensors dry is observed. This noise is reduced as the sweat starts closing the electrical contact between the electrodes. Once the volunteer starts sweating, the noise level is reduced down to levels of less than 0.5 mV (standard deviation of the baseline). In all the tested volunteers, the values obtained fall within the range of 0.1 to 1 mM NH_4^+ , which is close to the expected normal range.⁶ When the subject starts sweating, an increase of the levels of ammonium can be seen when the subject is increasing the load without any sprint (Fig. 5C left) and an increase of the signal while exercising due to increasing

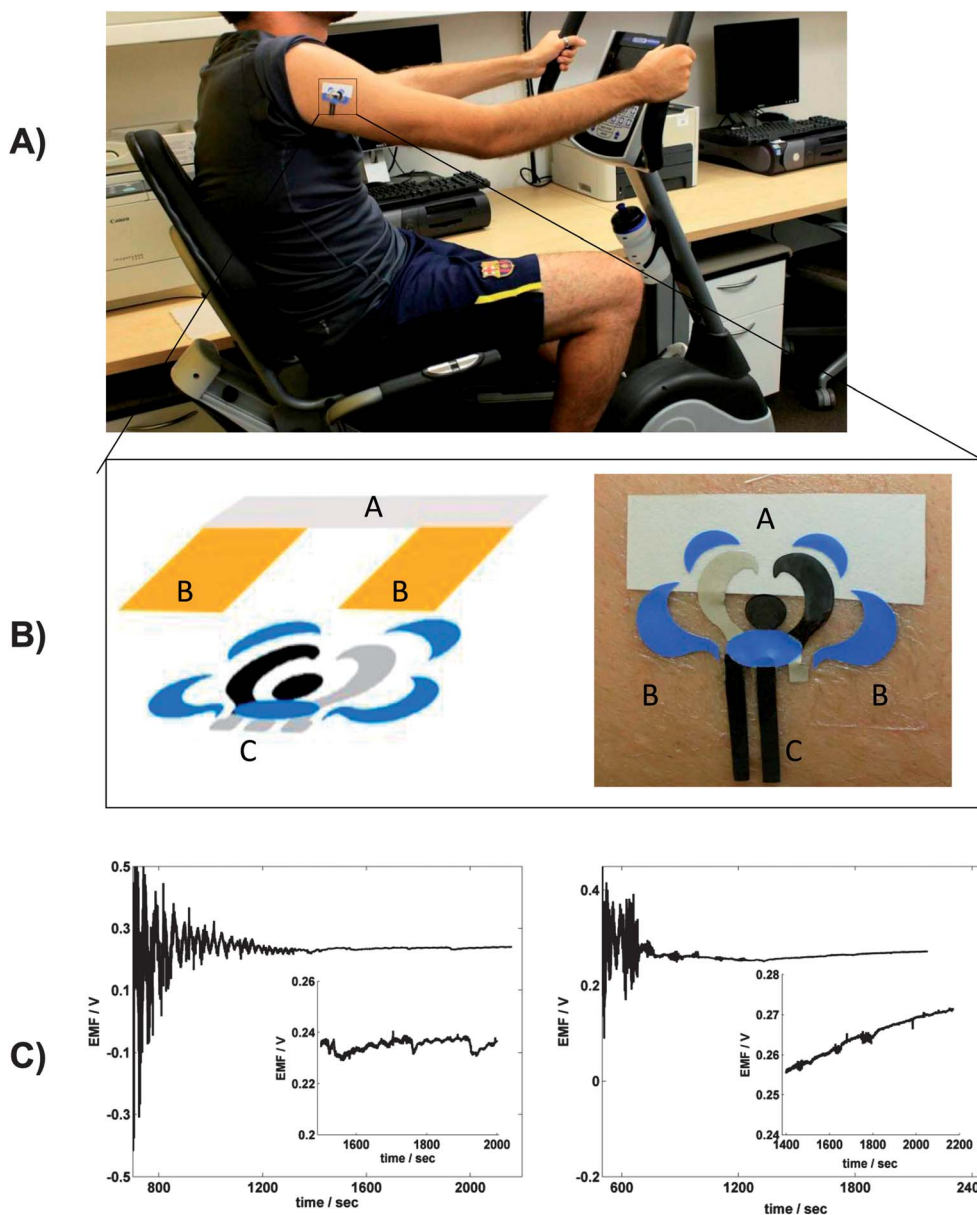


Fig. 5 On-body ammonium measurements. (A) Sensing tattoo placed on the shoulder. (B) Final design of the tattoo in order to facilitate a path where sweat can flow. Left: scheme of the fabrication of the path: A is the filter paper; B is Kapton and C connections. Right: overview of the tattoo placed on the skin: A is the filter paper, B is the Kapton (transparent) and C is the connections (PET carbon). (C) Real-time data obtained from a human volunteer. The stable section corresponds to the onset of sweat of the volunteer. Left: subject only increasing the load. Right: subject sprinting every 5 minutes.

the speed every 5 min (Fig. 5C right). This correlates with the switch from aerobic to anaerobic states. Future efforts will test the sensor at longer sprints, different speeds and different diets.

For on-body tests, a larger version of the tattoo was used in order to avoid the damage of the sensor while exercising (as it was observed previously in the stretching test and even in the initial trials of on-body tests) since a sharp drop of potential was observed while the volunteer was exercising on the cycle.

4. Conclusions

A new solid-state tattoo potentiometric cell to sense ammonium (NH_4^+) in sweat by combining screen-printed technology on a

temporary transfer tattoo has been introduced. This cell design introduces improvements to a polyvinyl-butyl (PVB) solid-state reference membrane that is used for the first time on a wearable device. The performance of this new sensor is comparable to conventional potentiometric electrodes, and it allows NH_4^+ sensing in sweat at physiological levels. This cell design does not show hysteresis effects and it presents extremely good resistance to mechanical stress. Preliminary results suggest that this ISE-tattoo can sense the change from aerobic to anaerobic state of subjects performing intensive exercise. While further tests are needed to fully exploit and validate the new epidermal ammonium sensor, the device opens up new avenues in monitoring sports performance,

healthcare, *etc.* Such coupling of the epidermal integration, screen-printed technology and potentiometric sensing represents an attractive path towards non-invasive monitoring of a variety of sweat electrolytes.

Acknowledgements

The authors acknowledge the financial support from the European Union, Marie Curie Grant PCIG09-GA-2011-293538 (Project FlexSens), Fundación Recercaixa (Project SensAge), the US National Science Foundation (Awards CBET-1066531), and the Spanish Ministry of Science and Innovation (MICINN), Ramón y Cajal program and project grant CTQ2010-18717, as well as Ministry of Economy and Competitiveness, FPI fellowship (BES-2011-048297) and also the additional financial support from EEBB-I-13-05936. J.R.W. acknowledges UCSD William J. von Liebig Center under the DOE-sponsored Southern California Clean Energy Technology Acceleration Program. The authors also thank Denise Molinnus for her help and valuable discussions.

References

- 1 K. Sato, W. H. Kang, K. Saga and K. T. Sato, *J. Am. Acad. Dermatol.*, 1989, **20**, 537–563.
- 2 W. N. Fishbein, J. W. Foelimer and J. I. Davis, *Int. J. Sports Med.*, 1990, **11**, S91–S100.
- 3 G. Ravier, B. Dugué, F. Grappe and J.-D. Rouillon, *Int. J. Sports Med.*, 2005, **26**, 1–8.
- 4 D. B. Shawcross, S. S. Shabbir, N. J. Taylor and R. D. Hughes, *Hepatology*, 2010, **51**, 1062–1069.
- 5 S. W. Brusilow and E. H. Gordes, *Am. J. Physiol.*, 1968, **214**, 513–517.
- 6 D. Czarnowski, J. Górski, J. Józwiuk and A. Boron-Kaczmarzka, *Eur. J. Appl. Physiol.*, 1992, **65**, 135–137.
- 7 P. Colombani, S. Späti, C. Spleiss, P. Frey-Rindova and C. Wenk, *Z. Ernährungswiss.*, 1997, **36**, 237–243.
- 8 D. Czarnowski and J. Górski, *J. Appl. Physiol.*, 1991, **70**, 371–374.
- 9 Y. Yuan and K.-M. Chan, *Br. J. Sports Med.*, 2004, **38**, 115–119.
- 10 I. Alvear-Ordenes, D. García López, J. A. De Paz and J. González-Gallego, *Int. J. Sports Med.*, 2005, **26**, 632–637.
- 11 D. Czarnowski, J. Langfort, W. Pilis and J. Górski, *Eur. J. Appl. Physiol.*, 1995, **70**, 70–74.
- 12 B. Schazmann, D. Morris, C. Slater, S. Beirne, C. Fay, R. Reuveny, N. Moyna and D. Diamond, *Anal. Methods*, 2010, **2**, 342–348.
- 13 V. F. Curto, C. Fay, S. Coyle, R. Byrne, D. Diamond and F. Benito-López, *15th International Conference on Miniaturized Systems for Chemistry and Life Sciences*, October 2–6 2011, pp. 577–579.
- 14 S. Coyle, *et al.*, *IEEE Trans. Inform. Tech. Biomed.*, 2010, **14**, 364–370.
- 15 Y.-L. Yang, M.-C. Chuang, S.-L. Lou and J. Wang, *Analyst*, 2010, **135**, 1230–1234.
- 16 K. Malzahn, J. R. Windmiller, G. Valdés-Ramírez, M. J. Schöning and J. Wang, *Analyst*, 2011, **136**, 2912–2917.
- 17 T. Guinovart, M. Parrilla, G. A. Crespo, F. X. Rius and F. J. Andrade, *Analyst*, 2013, **138**, 5208–5215.
- 18 D.-H. Kim, N. Lu, R. Ma, Y.-S. Kim, R.-H. Kim, S. Wang, J. Wu, S. M. Won, H. Tao, A. Islam, K. J. Yu, T.-I. Kim, R. Chowdhury, M. Ying, L. Xu, M. Li, H.-J. Chung, H. Keum, M. McCormick, P. Liu, Y.-W. Zhang, F. G. Omenetto, Y. Huang, T. Coleman and J. A. Rogers, *Science*, 2011, **333**, 838–843.
- 19 J. R. Windmiller, A. J. Bandodkar, G. Valdés-Ramírez, S. Parkhomovsky, A. G. Martínez and J. Wang, *Chem. Commun.*, 2012, **48**, 6794–6796.
- 20 W. Jia, G. Valdés-Ramírez, A. J. Bandodkar, J. R. Windmiller and J. Wang, *Angew. Chem., Int. Ed.*, 2013, **52**, 7233–7236.
- 21 A. J. Bandodkar, V. W. S. Hung, W. Jia, G. Valdés-Ramírez, J. R. Windmiller, A. G. Martínez, J. Ramírez, G. Chan, K. Kerman and J. Wang, *Analyst*, 2013, **138**, 123–128.
- 22 T. Guinovart, G. A. Crespo and F. J. Andrade, submitted.
- 23 M. S. Ghauri and J. D. R. Thomas, *Anal. Proc.*, 1994, **31**, 181.
- 24 E. A. Guggenheim, *J. Phys. Chem.*, 1929, **33**, 842–849.
- 25 C. Harvey, R. Lebouf and A. Stefaniak, *Toxicol. In Vitro*, 2010, **24**, 1790–1796.
- 26 F. X. Rius-Ruiz, G. A. Crespo, D. Bejarano-Nosas, P. Blondeau, J. Riu and F. X. Rius, *Anal. Chem.*, 2011, **83**, 8810–8815.